Turk J Chem
23 (1999) , 381 – 391.

Electrochemical Characterization of Al_2O_3-Ni Thin Film Selective Surface on Aluminium

Figen KADIRGAN
Department of Chemistry, İstanbul Technical University,
Maslak 80626, İstanbul-TURKEY
Ewa WACKELGARD
TÜBİTAK, Marmara Research Centre,
P.O. Box 21, 41470 Gebze, Kocaeli-TURKEY
Mete SÖHMEN
Solid State Physics, Uppsala University,
Teknikum, Box 534, S-75121 Uppsala-SWEDEN

Received 07.04.1999

Solar thermal collectors represent a widely used type of system for the conversion of solar energy. In order to produce selective coatings on aluminium substrates to be used as absorber plates in high efficiency solar collectors, nickel pigmentation was applied to anodically oxidised surfaces. Electrochemical dc methods are used to study the oxidation of aluminium as functions of the following electrolysis conditions: applied current, pH, temperature and concentration of electrolyte. The properties of the oxidised aluminium surfaces are investigated by cyclic voltammetry. Nickel pigmentation of porous aluminium surfaces was also performed as a function of electrochemical pigmentation conditions by ac electrodeposition. Mechanisms contributing to selectivity in anodically oxided aluminium and electrodeposits are discussed. The optical properties of the prepared surfaces are optimised, and solar absorptance α_s=0.91 and thermal emittance $\epsilon_{t,23^\circ C}$=0.17 are obtained.

Introduction

Thin film surface coatings are widely used for efficient conversion of solar radiation into useful forms, notably thermal energy for heating and cooling applications in both active and passive systems. Material performance, ease of manufacture and resistance to lifetime limiting degradation are crucial to the economic success of photothermal solar energy conversion. High absorption over the solar radiation spectrum and low emittance in the thermal infrared must be provided in a thin film with low manufacturing and material cost. One of the appropriate techniques for obtaining an absorber coating with selective optical properties for solar collectors is electrodeposition (1-7). One of the most frequently used commercial materials in solar absorbers is nickel pigmented aluminium oxide on aluminium. The production cost of this coating is low and it has fairly good selective properties and is quite resistant to degradation.

Experimental

Samples consisting of 3×2 cm pieces were cut from flat sheets of commercial grade aluminium. After thorough rinsing, the samples were subjected to a chemical polishing treatment consisting of alkaline (NaOH) and acid etchants (H_3PO_4 and H_2SO_4). Anodization was achieved using a classical double-walled three-electrode cell coupled to an EG&G 273 Potentiostat-Galvanostat system at constant current in phosphoric acid solution. After anodization, the samples were neutralised for 10 minutes in sodium bicarbonate in order to remove the residual phosphoric acid. Pigmentation was achieved using nickel sulfate salts at a constant temperature of 20° C.

Optical reflection/emission properties of the samples were characterised. In the visible range we used a Jasco V500 spectrophotometer equipped with an ILN-472 integrating sphere. In the IR region we used a Jasco FTIR/700 and RSA-FTIR 6 inch integrating sphere combination. The reflectance of the samples was recorded with a gold coated integrated sphere. A gold reference was used as a standard.

Results and Discussion

Potential-time transient behaviour of aluminium oxidation:

The oxide formed in the initial stages of porous oxide growth and that which remains interposed between the pore-containing layer and the metal is often referred to as a barrier layer. The voltage-time (E-t) curves resulting from anodic oxide formation of aluminium is critically dependent on the concentration of phosphoric acid H_3PO_4, temperature and applied current.

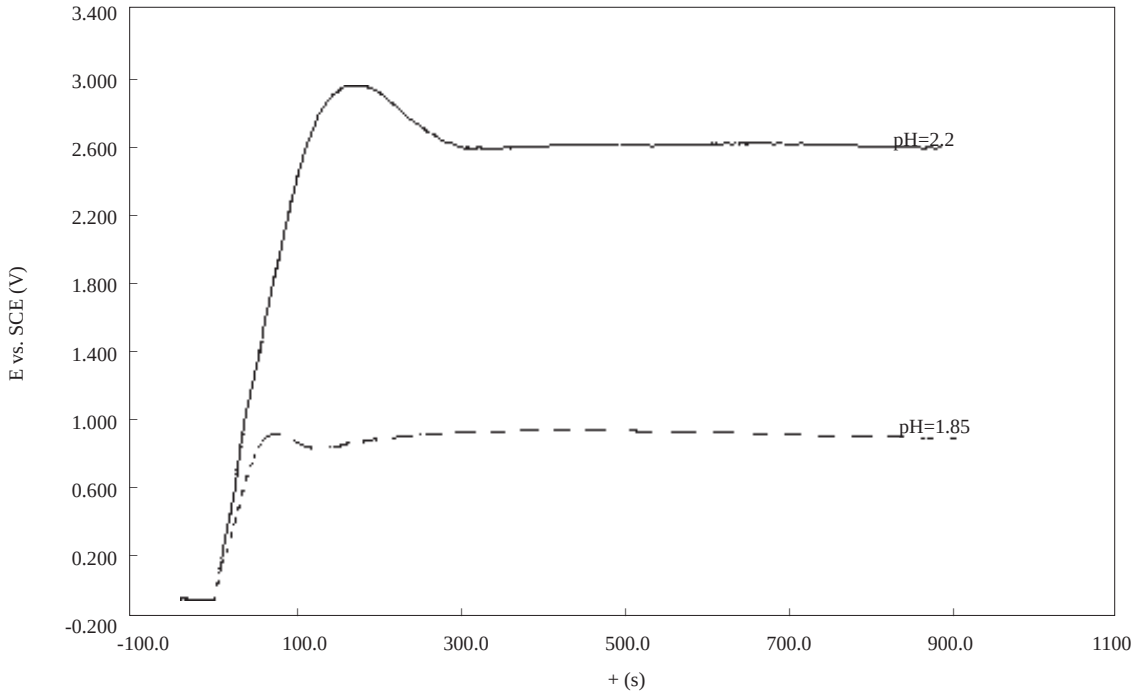

Figure 1. E-t curves in function of pH (I_{app}=30 mA, t=900 s., T=25° C)

-2 M H_3PO_4 ...2.5 M H_3PO_4

Influence of the pH

Fig. 1 shows the effect of pH at constant time and current on the anodic potential as a function of anodising time. The potential maximum occurs between 60 sec. and 150 sec. depending on pH and anodising time, and attains the steady-state value between 120 and 300 sec. The potential maximum in pore-forming environments is seen to correspond to pore initiation in accordance with the postulation that initiation does not occur until the field has dropped to a level that permits proton entry into the film. The subsequent decrease in leakage potential reflects the thinning of the barrier layer in the bottom of the pores as pore growth proceeds. The steady-state potential reflects stability of the barrier film (10 Å V^{-1}) and pore growth occurring by growth of the film. Pore growth is 10Å V^{-1} at 25°C. As is seen in Fig.1, as the $[H^+]$ is increased, the potential maximum decreases and a steady-state value is obtained in a shorter time. This may be explained by the chemical dissolution of the barrier oxide layer.

Influence of the temperature

The effect of temperature on the anodic film formation of aluminium is shown in Fig. 2 for constant current and pH. With increasing temperature, the potential maximum increases and the barrier layer grows thicker. Also, the potential drops rapidly after the formation of pores. This effect is more pronounced at higher temperatures.

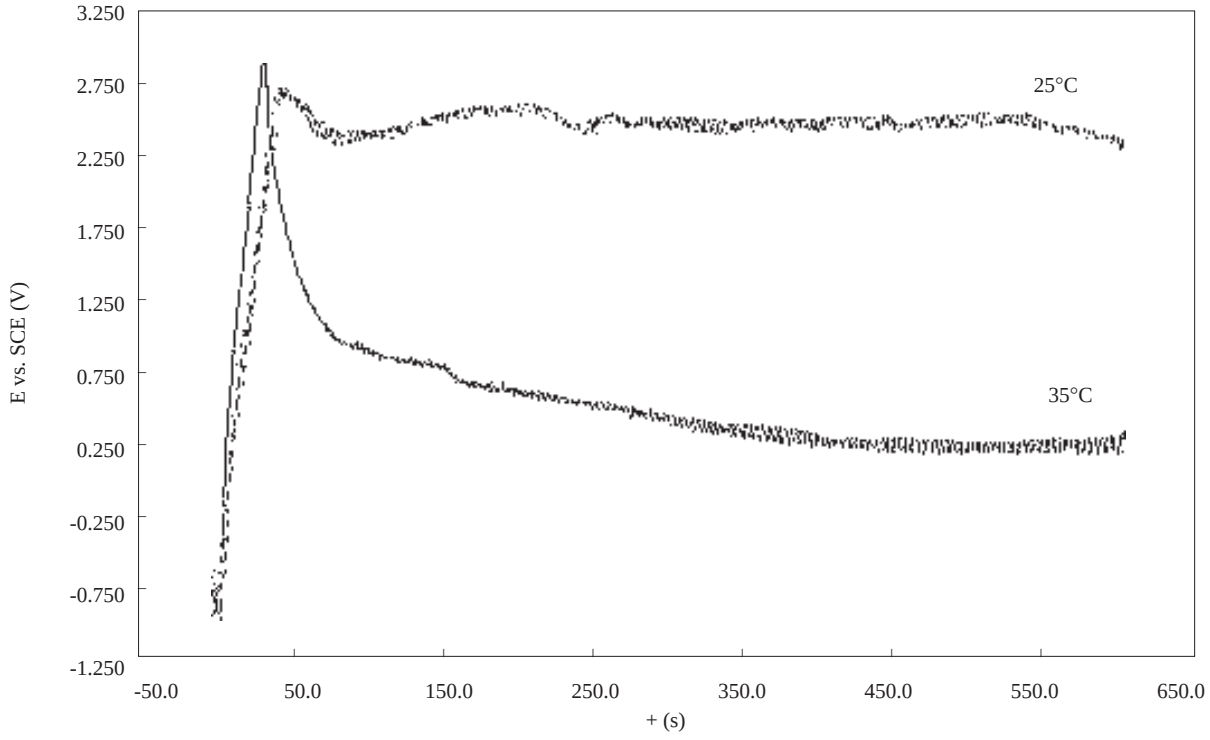

Figure 2. E-t curves in function of temperature (I_{app}=8 mA, 2 M H_3PO_4, t=600 s.)

– 25° C ...35 °C

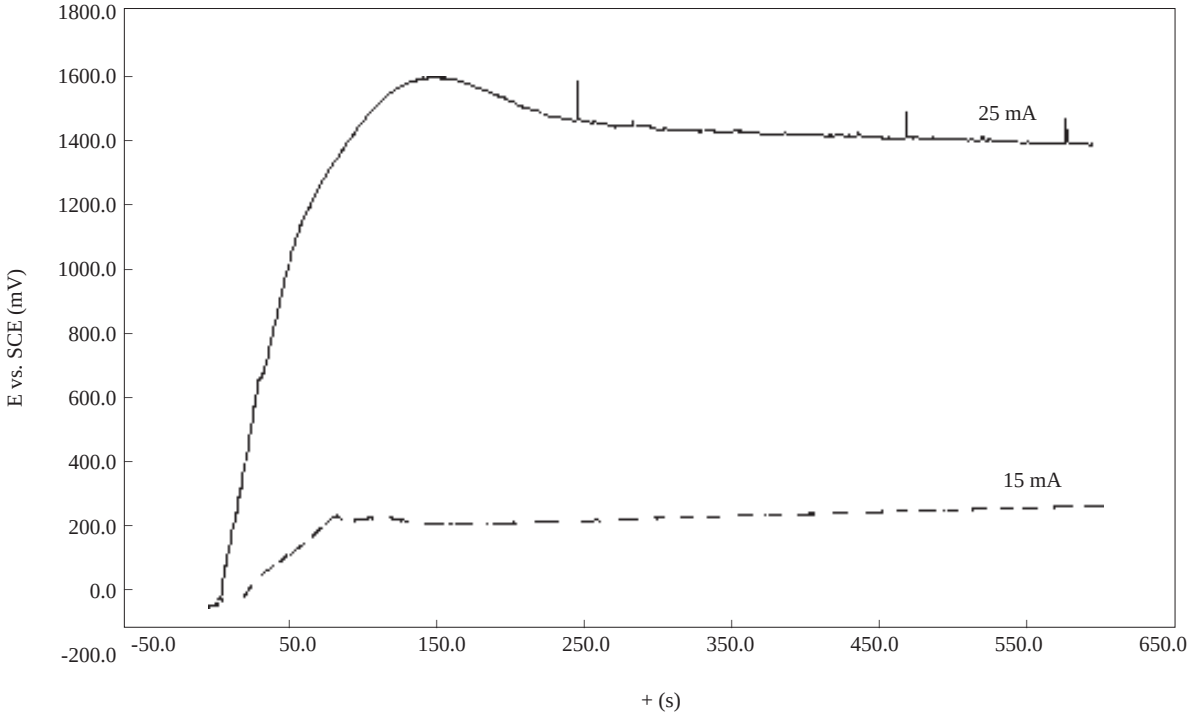

Figure 3. E-t curves in function of applied current (2 M H_3PO_4, T=25° C, t=600 s.)

-I_{app}=25 mA ... I_{app}= 15 mA

Influence of applied current

It is shown in Fig. 3 that with increasing current, the potential maximum increases and a steady state value occurs for a longer time. This effect may also be due to the formation of a more compact oxide layer at a higher current.

The voltametric properties of aluminium and aluminium oxide

First, a cyclic voltammogram of polished aluminium plate was taken before and after different oxidation processes to observe coating corrosion behaviours. It is well known that the aluminium surface easily oxidizes in air and in water. The corrosion behaviour of aluminium is determined by the behaviour of the covering oxide film. Poor resistance to corrosion is often connected with a change in this oxide film, notably in its degree of hydration and porosity. However, after polishing treatment, we took the I-V curves of aluminium in the 2.3 M H_3PO_4 solution, varying some experimental parameters such as the potential range for aluminium oxidation and the rate of the potential sweep. We noted that each parameter has changed for a new polished material, and the first cycle was studied to avoid the oxidation as much as possible.

The voltametric I-E curves show that the dissolution or hydration of aluminium in acid medium starts at a negative potential (-0.55 V vs. SCE). The reaction rate increases at a more positive potential, reaching its maximum value at -0,40 V vs. SCE. During the negative variation of potential, the electrode sites are almost blocked by the surface oxide layer until the reduction/dehydration takes place at very negative potential values. For our films, this reduction takes place at -0.5 V vs. SCE, reaching a negative current

peak at -0.65 V (Fig. 4). The difference between oxidation and reduction peak potential's is more than 100 mV, which means that the redox reaction is irreversible.

The effect of varying the upper potential sweep limits is shown in Fig. 5, from which it can be seen that decrease of the upper limit leads to an increase on the intensity of the oxidation/dissolution peak of aluminium. This may be due to the increase in the oxidized surface, which is not completely reduced at higher values of the upper potential limit.

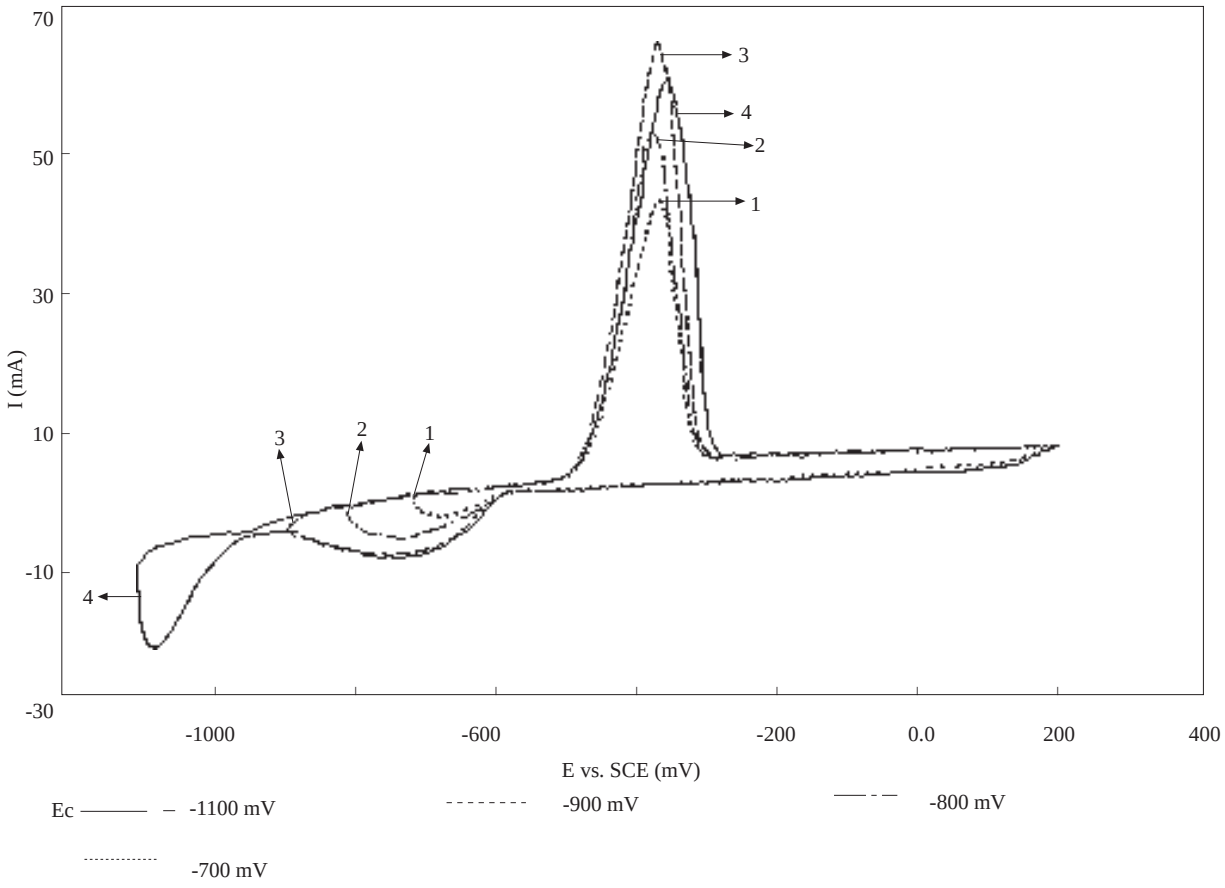

Figure 4. Effect of varying the lower potential limit of unoxidized Al.

(2.5 M H_3PO_4, T=25° C, v=50 mV/s.)

1.E=-700 mV 2.E=-800 mV 3.E=-900 mV

4.E=-1100 mV vs. SCE.

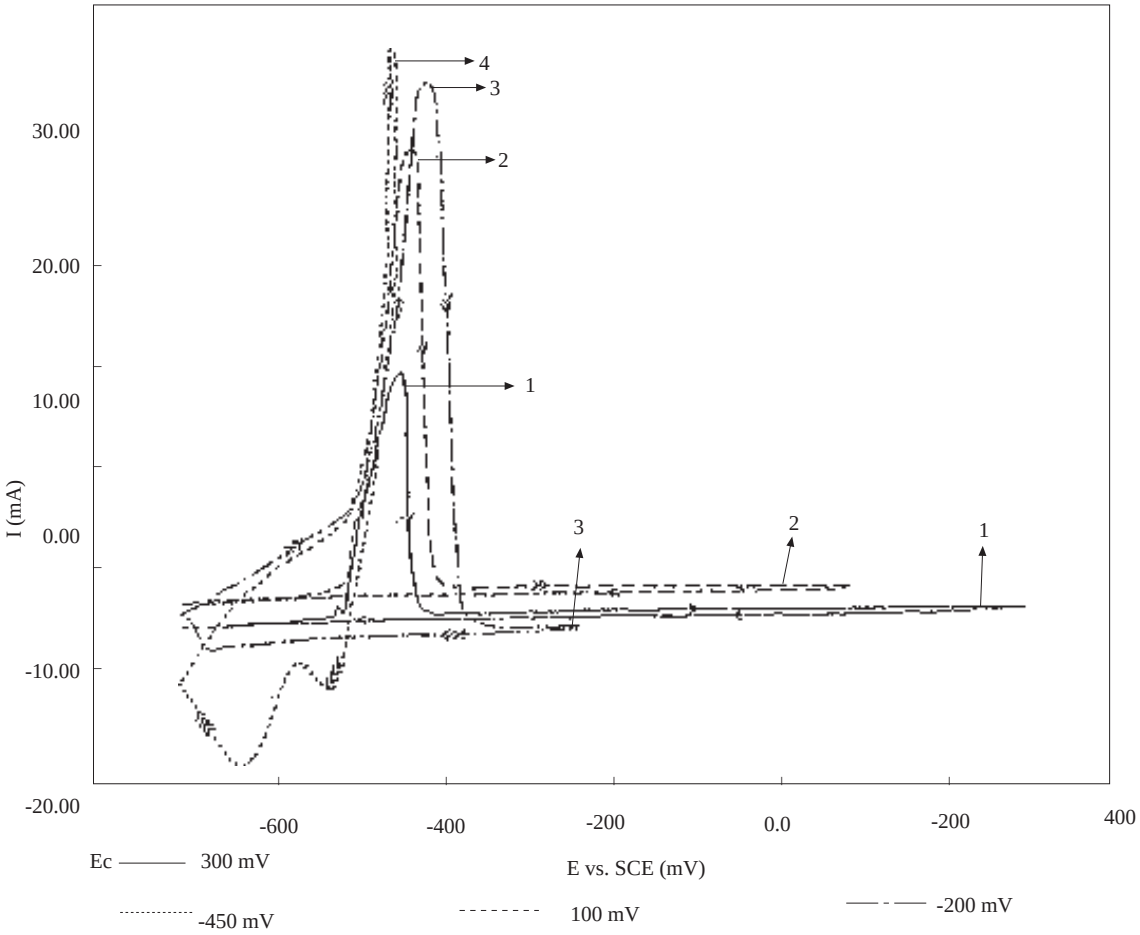

Figure 5. Effect of varying the upper potential limit of unoxidized Al.

(2.5 M H_3PO_4, T=25° C, v=50 mV/s.)

1.+300 mV 2.+100 mV 3-200 mV -450 mV vs. SCE

On an oxidized aluminium surface, by varying the upper potential sweep limits, one can observe the same behaviour. The peak potentials were at more positive potentials (-300, -350 mV vs. SCE). As the negative limits are varied, the current density of the dissolution peak slightly decreases at higher positive limits. This may be explained by the reduction of the surface at more negative potentials.

To see the effect of the oxide layer preparation condition on the I-E curves of aluminium, the I-E curves of the oxidised aluminium at different pH and applied current are investigated. Decreasing the pH during oxide preparation results in a higher current density of the dissolution peak (Fig. 6). The increase in the current density at lower pH values may be due to weak pore formation on the surface during the oxidation process. The I-E curves show the effect of applied current on oxide formation (Fig. 7). As the applied current increases, the dissolution peak becomes higher on the I-E curve. This may be due to the formation of a more compact oxide with higher current values. The effect of varying the sweep rate (v) of the voltage sweep at constant potentials is examined both for oxidized and unoxidized aluminium surfaces. The current density of the peak stays constant with $\sqrt{\nu}$ for sweep rates < 50 mVs^{-1} where they become independent

of (v) for higher than 1000 mVs^{-1} sweep rates. This effect is seen both for oxidized and unoxidized surfaces (Fig.8).

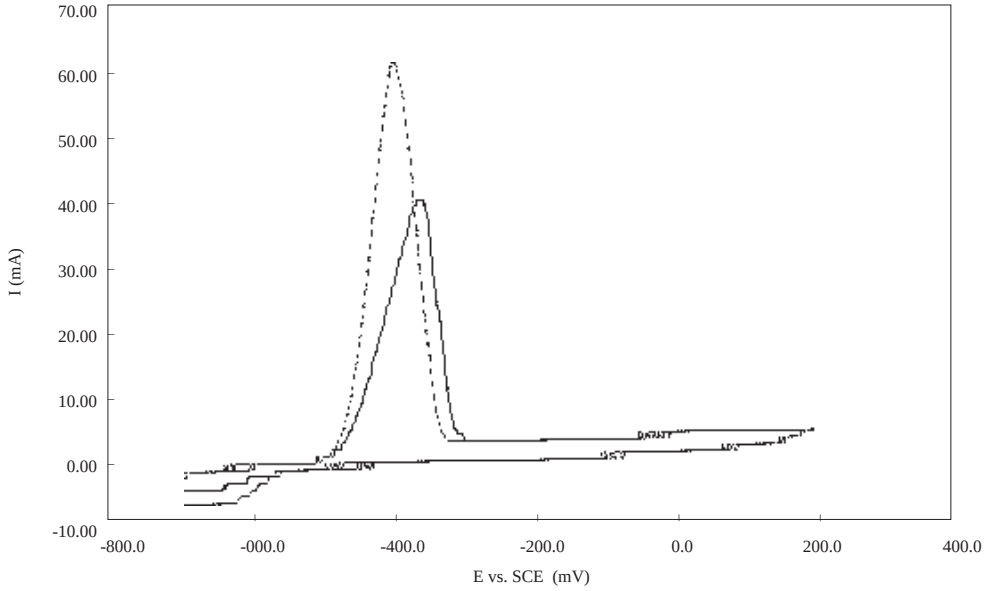

Figure 6. Cyclic voltammograms of oxidised aluminium in two different concentrations of the electrolyte. (2.5 °C, v=50 mV/s.)

.....2 M H_3PO_4 ——2.5M H_3PO_4

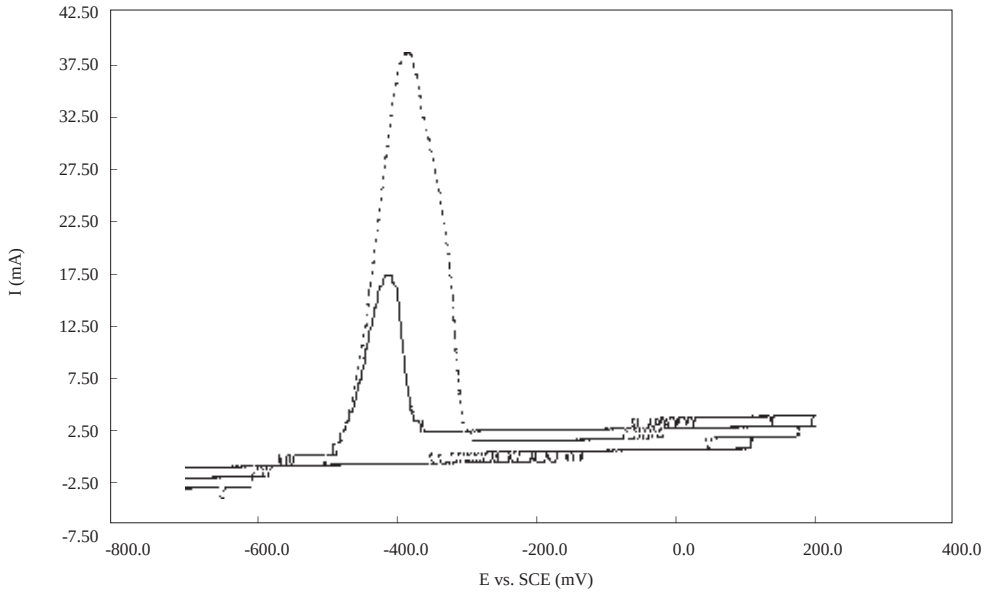

Figure 7. Cyclic voltammograms of oxidised aluminium at two different applied current values. (T=25 °C, v=50 mV/s, 2.5 M H_3PO_4)

.....6 mA ——4 mA

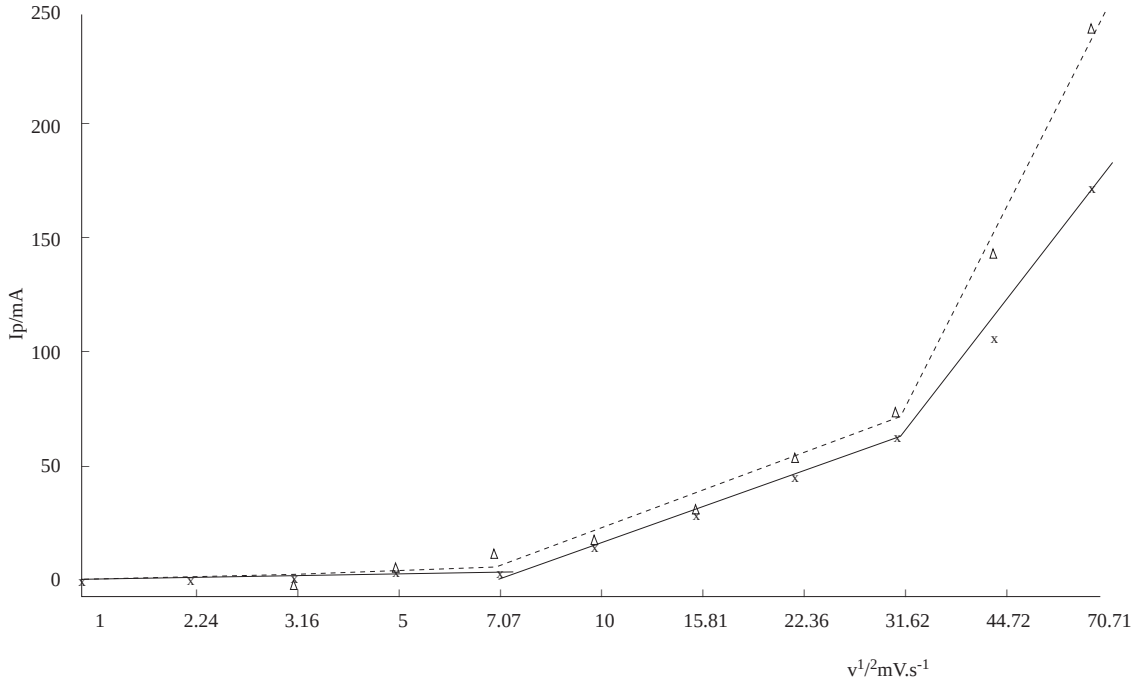

Figure 8. Peak current dependence vs. square root of scan rate at the aluminium electrode. (2.5 M H_3PO_4, 25 °C)

xxx unoxidised aluminium ΔΔΔ oxidised aluminium at 4 mA

In the case of diffusion and charge transfer controlling the rate of reaction, the peak potential, E_p, varies with the sweep rate according to

$$E_p = E_0 + b'(0.78 + (ln(D_0/b')^{1/2}) + lnv^{1/2} - lnks) \tag{1}$$

where

$$b' = RT/nF \tag{2}$$

E_0 being the standard potential, D_0 the diffusion coefficient, n the number of electrons per molecule oxidized or reduced, R the gas constant, T the absolute temperature and k_s the heterogeneous rate constant at the standard potential. The equation can be simplified as follows:

$$E_p = \frac{1}{2}blogv + const \tag{3}$$

where

$$b = 2.303b' \tag{4}$$

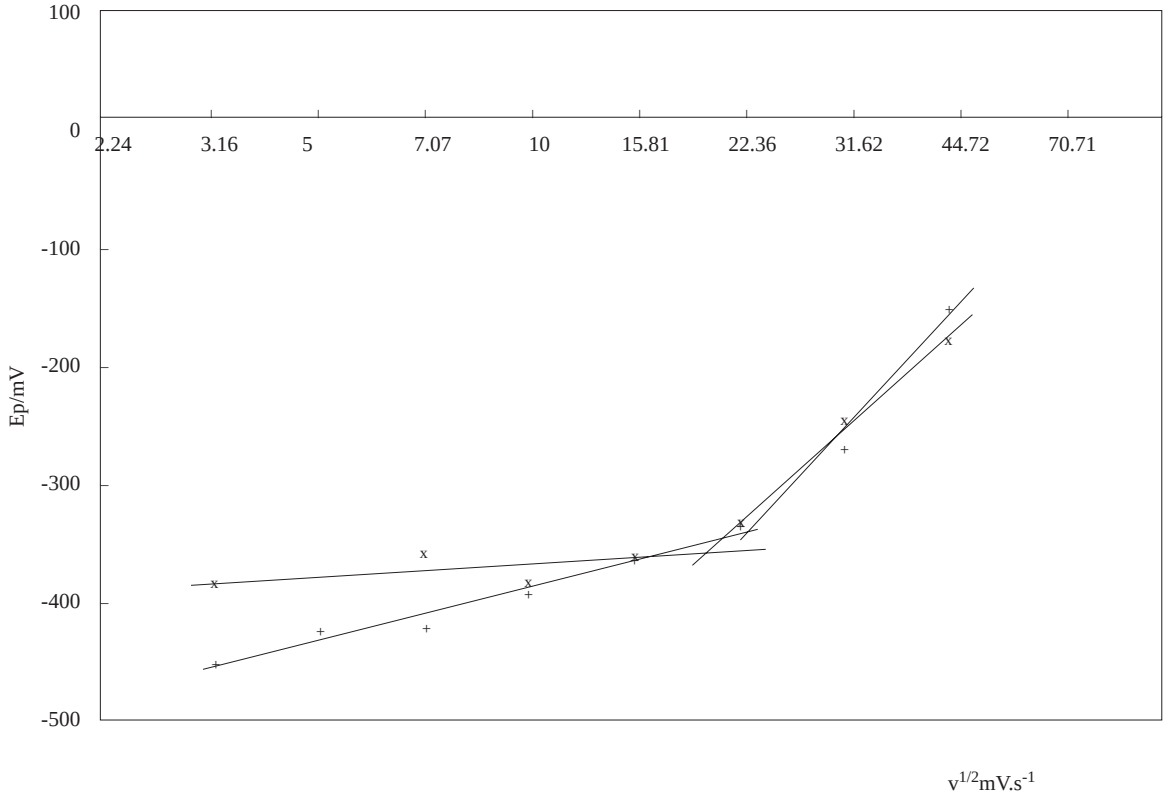

Figure 9. Peak potential dependence vs. square root of scan rate at the aluminium electrode. (2.5 M H_3PO_4, 25 °C)

xxx unoxidised aluminium ++++ oxidised aluminium at 4 mA

and all constant terms have been summarised into the single constant. Fig. 9 represents plots of E_p vs. $v^{1/2}$ mVs^{-1} for both the oxided and unoxided surface. From the slopes, it is seen that on the unoxided surface the peak potentials are independent of the sweep rate of the potential up to 250 mVs^{-1}. This means that charge transfer does not control the dissolution reaction. The slopes obtained from $\frac{\partial E}{\partial log v}$ are 0.3 mV (when $v < 150$ $mV.s^{-1}$) and 6.66 mV (when $v > 150$ $mV.s^{-1}$) for unoxidised aluminium. The slopes are 6.59 mV (when $v < 150$ $mV.s^{-1}$) and 8.14 mV (when $v > 150$ $mV.s^{-1}$) for the oxidized aluminium surface. Therefore, the values for the Tafel slope of b are 0.6 mV and 13.32 mV/decade for unoxidized aluminium and 13.18 mV and 16.28 mV/decade for oxidized aluminium. The constant is determined from the intercept.

We determined the optimum operating conditions under which a spectrally selective surface of nickel pigmented aluminium occurs. the spectral reflectance and thermal emittance of nickel pigmented aluminium was studied as a function of applied current of aluminium oxide layer and nickel pigmentation time. The following standard experimental conditions were used in preparing the samples for reflectance-emittance measurements.

Anodic oxidation bath conditions

Bath concentration: 1.5-2.5 M H_3PO_4,

Current density: 0.1-0.25 A/dm^2 or 0.25-0.40 A/dm^2

Bath temperature: 15-25 °C

Deposition time: 8-20 minutes

Nickel pigmentation bath conditions:

Bath concentration: 0.2-1.4 M $NiSO_4.7H_2O$+0.25-1.5 M H_3BO_3

Bath temperature: 15-25 °C

Potential applied: 10-20V

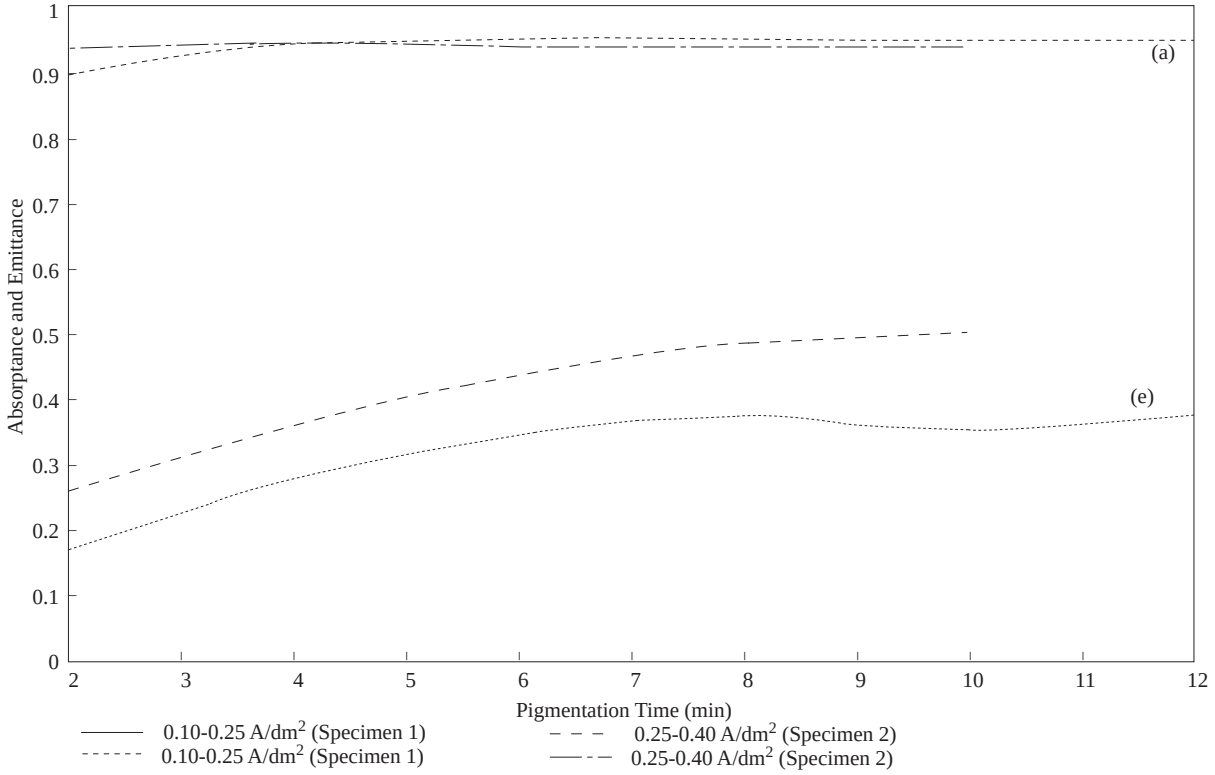

Figure 10. Spectral reflectance, absorptance (a) and emittance (e) profiles of nickel pigmented aluminium oxide specimens. (Bath conditions are given in page 7)

——— (e) profiles of aluminium which is oxidised at 0.1-0.25 A/dm^2

-.- (e) profiles of aluminium which is oxidised at 0.25-0.4 A/dm^2

— (a) profiles of aluminium samples which are oxidised at both conditions

Fig. 10 shows the solar absorptance α_s and emittance ϵ_t values calculated from the reflectance spectra. The data indicates that specimen 1 has better optical characteristics at short pigmentation times, which can be explained by difference in the thickness of the aluminium oxide layer on the optical properties of

the deposit. The absorbing region attains a steady-state value after 5 min. nickel deposition time. However, the emittance values increase with the deposition time.

Conclusion

The effects of pH, temperature and applied current on oxide thickness are observed. The data shows that increasing pH and temperature values result decreasing in oxide thickness. The emittance is increased with film thickness. High absorptance can be obtained for all oxide thicknesses according to the nickel deposition time. However, for good selectivity, the oxide layer should not be completely pigmented (8). An improvement in emittance is obtained for shorter nickel deposition times. The optical properties of the prepared surfaces are optimised, and a solar absorptance of 0.91 and a thermal emittance of 0.17 are obtained (2).

References

1. F. Kadırgan, M. Söhmen, İ. E. Türe, Ş. Süzer, J. Wetherilt, A. Yazar, *Renewable Energy,* 10 No.2/3, 203-206, (1997).
2. F. Kadırgan, M. Söhmen, İ. E. Türe, J. Wetherilt, Turkish Patent, Submitted, No: 96/00599, 1996.
3. A. Ross, M. Georgson, E. Wackelgard, Solar *Energy Materials*, 22, 15-18 (1991).
4. O. T. İnal, A. Scherer, *J. Materials Science,* 23, 1934-1942 (1986).
5. Andersson, A. O. Hunderi, C. G. Granqvist, *J. Applied Physics*, **51**, 745-764 (1980).
6. E. Wackelgard, T. Chibuye, B. Karlsson, *Energy Conversion In Buildings,* 177-182, Pergamon Press, Oxford, (1990).
7. T. Pavloic, A. Ignatiev, *Solar Energy Materials,* 16, 319-331 (1987).
8. S. Süzer, F. Kadırgan, H. M. Söhmen, A. J. Wetherilt, İ. E. Türe, Solar Energy and Solar Cells, 52, 55-60 (1998).